

## THE FABRICATION OF POROUS HYDROXYAPATITE SCAFFOLD USING GAUR GUM AS A NATURAL BINDER

J. ANITA LETT<sup>a\*</sup>, M. SUNDARESWARI<sup>a</sup>, K. RAVICHANDRAN<sup>b</sup>,  
S. SAGADEVAN<sup>c</sup>

<sup>a</sup>*Department of Physics, Sathyabama Institute of Science and Technology,  
Chennai-600 119, Tamil Nadu, India*

<sup>b</sup>*Department of Analytical Chemistry, University of Madras, Chennai- 600025,  
Tamil Nadu, India*

<sup>c</sup>*Centre for Nanotechnology, AMET University, Chennai-603 112, India*

In bone tissue engineering, Hydroxyapatite (HA) is extensively used in medical applications as an implant material to enhance bone growth formation or as drug release vehicle because of its resemblance to the components of human bones and for its excellent biocompatibility. The porous structure is generally used as a scaffolding material. Many techniques have been applied to fabricate HA porous scaffolds. In this work, polymeric sponge technique was employed in the preparation of HA scaffold, using gum Ghatti, a natural binder obtained from the barks of *Anogeissus latifolia* species. The influence of binder concentration for various sintering temperature 1100 °C, 1150 °C and 1200 °C was estimated. The Hydroxyapatite starting powder and Hydroxyapatite scaffold were characterized for phase purity, structural analysis, porosity measurements and mechanical properties. It is possible to produce Hydroxyapatite scaffolds with highly inter connecting macro ranging from 500 to 1000 µm and micro pores from 400 to 2000 nm with a compressive strength ranging from 0.43 MPa to 2.62 MPa, comparable to trabecular bone.

(Received November 12, 2017; Accepted February 15, 2018)

*Keywords:* Hydroxyapatite scaffolds, natural gum, gaur gum, compressive strength.

### 1. Introduction

Bone scaffoldings are used for formation of new bone in circumstances such as restoration of skeletal fractures between two bones, to compensate and reestablish lost bone, infection or disease, or to improve the bone mending response and reconstruction of bone tissue in the vicinity of surgical implants like artificial hinge restoration or plates and screws. The best way is to achieve bone scaffoldings in use of osteophilic material. Application of porous materials are especially biocompatible, osteoconductive and osteointegrative, which means that the new tissue and eventually fresh cells can be induced to grow into the pores which help to enhance strong fixture with the scaffolding materials [1]. Additionally, well-suited mechanical strength is important to provide structural support for load bearing applications. Amongst the various materials, HA has been widely used as bone graft and could be a potential aspirant of choice due to its close acquaintance with similar inorganic mineral constituent present in the hard tissues of natural bone and teeth and offers excellent biocompatibility and bioactivity [2]. Moreover, bone and tooth implants such as titanium and its alloys have been coated with HA to strengthen its osteointegration with the host tissue [3].

In the phenomenon of bone scaffolding, synthetic hydroxyapatite is frequently used to perform exclusive aspects in regeneration and restoration of damaged parts. These scaffolds involve in promoting cell-biomaterial interaction, cell-adhesion, transporting vital nutrients, bone cell proliferation and differentiation etc. An ideal scaffold should possess biodegradability and lower toxicity besides having appropriate strength, porosity and microstructure. The outstanding

---

\* Corresponding author: janitalett17@gmail.com

physical and biological properties associated with HA make an innate option for the scaffold application. However, the compositional similarity and three dimensional interconnected porous structures are necessary to perform cell attachment, proliferation, differentiation and to maintain circulation of bio-fluids at the damaged areas [4]. The biological response of these scaffolding materials are improved through the incorporation of collagen, Chitosan, etc, [5]. Several binders both natural and synthetic have been investigated. In the preparation of HA scaffolds, the binding ability of starch [6], gelatine [7,8], gelatin / polyvinyl alcohol composites[9] have already been studied and we have also reported the works done on cellulose, starch and PVA as a binding agent [10, 11]. For a bio-ceramic the ideal pore size should be comparable to that trabecular bone. It has been confirmed that micro porosity (pore size < 10  $\mu\text{m}$ ) allows body fluid circulation whereas macro porosity (pore size > 50  $\mu\text{m}$ ) provides scaffold for bone-cell colonization [31]. The highly interconnected porous structure of HAP seems to be a potential candidate for the environment of posterolateral lumbar with higher cellular viability [12].

In the present study, highly porous HAP scaffolds with highly interconnecting macro pores (500 – 1000  $\mu\text{m}$ ) and micro pores(400 – 2000 nm) were prepared using a simple method employing spongy technique using a natural binder guar gum. Guar gum, also called guaran, obtained from *Anogeissus latifolia* Wall (family Combretaceae). It is primarily the ground endosperm of guar beans. The guar seeds are de-husked, milled and screened to obtain the guar gum. It is typically produced as a free-flowing, off-white powder. Guar gum can best be described as a natural food thickener, similar to locust bean gum, cornstarch or tapioca flour. It is said to have significantly more thickening ability than cornstarch and a popular additive in puddings and ice creams. Chemically, guar gum is a polysaccharide composed of the sugars galactose and mannose. The backbone is a linear chain of  $\beta$  1,4-linked mannose residues to which galactose residues are 1,6-linked at every second mannose, forming short side-branches[13]. In the current work, the binding ability of guar gum in the fabrication of HAP scaffolds was studied. It is found that by controlling the binder concentration and sintering temperature it is possible to produce HA scaffolds with compressive strength in the ranging from 0.43 MPa to 2.62 MPa, which can be preferred for non-load bearing applications. The bioactivity of these scaffolds was investigated by soaking them in simulated body fluid (SBF).

## **2. Experimental Procedure**

### **2.1. Synthesis of Hydroxyapatite Powder**

Analytical grade calcium nitrate tetra hydrate ( $\text{Ca}(\text{NO}_3)_2 \cdot 4\text{H}_2\text{O}$ ) and diammonium hydrogen phosphate ( $(\text{NH}_4)_2\text{HPO}_4$ ) from Sigma-Aldrich, were used as precursors for calcium and phosphate. Hydroxyapatite powders were synthesized by hydrothermal method based on the precipitation of HA particles from aqueous solution and ageing in high temperature and pressure. The synthesis procedure involved drop by drop addition of the  $(\text{NH}_4)_2\text{HPO}_4$  solution (0.6 M) into an aqueous suspension of  $\text{Ca}(\text{NO}_3)_2 \cdot 4\text{H}_2\text{O}$  (1 M) while maintaining the pH to 11 using ammonia solution and stirring at 500 rpm for 30 minutes. The final milky suspension was transferred to an autoclave and hydrothermally treated at 180  $^\circ\text{C}$  for 24 h. The resulting precipitates was washed and then oven dried at 100 $^\circ\text{C}$  for 20 hours and further calcinated in a muffle furnace at 800  $^\circ\text{C}$  for 2 hours. The final powder was characterized and used for the preparation of scaffolds.

### **2.2. Fabrication of Hydroxyapatite Porous Scaffold**

Scaffolds were prepared by sponge technique using synthesized HA powder as given in previous studies [14, 15]. Hydrothermally prepared nano crystalline hydroxyapatite powder of particle size smaller than 100 $\mu\text{m}$  was used. A natural gum ,guar gum obtained from the ground endosperm of guar beans, is used as a binding agent to prepare the scaffold. The binder of ratio 10 wt% and 15 wt% was mixed with water at 50  $^\circ\text{C}$  for 2hrs to form a homogenous mixture. To the mixture 5 ml of a tensioactive agent (A40 V ® Dispex provided from BASF) was blended for another 2 hrs to disperse thoroughly. Then, polyurethane sponges of appropriate size 10  $\times$  10  $\times$  10mm with an average pore size of roughly 500  $\mu\text{m}$  was dipped in the slurry several times, until

the void space was fully removed. The excess slurry was removed and the sponges were dried for 2 days at room temperature, followed by drying in a hot air furnace for 2 hrs.

After drying, the plunged polyurethane sponge was heat treated in a muffle furnace in two plateaus. First plateau at 600 °C for 2hrs to remove the polyurethane sponge, then followed by sintering for 4 hrs at 1100 °C, 1150 °C and 1200°C respectively for densification of scaffold. These were labelled as A1 1100 °C, A1 1150 °C, A1 1200 °C for 5 wt% and A2 1100 °C, A2 1150 °C, A2 1200 °C for 10 wt% gaur gum concentration. Finally, the scaffolds were allowed to cool gradually and cut into desired size for characterization.

### 2.3. Characterization techniques

The crystalline phase identification and phase purity determination of the calcined Hydroxyapatite powder and Hydroxyapatite scaffold were carried out by Philips X'pert Pro diffractometer, (Schmager, Netherlands) using nickel filtered  $\text{CuK}_\alpha$  radiation ( $k_\alpha = 1.5406 \text{ \AA}$ ). The samples were scanned from 10° to 80° (2theta) angle in steps of 0.0288983, with a count of 0.5 seconds at each point. The functional group identification of HA scaffolds, was carried out using a single beam Fourier transform infrared spectrometer (Agilent, Cary 630) in the spectral range from 4000 to 650  $\text{cm}^{-1}$ . Morphological micro and macro structural characterization were carried out on the samples using Field Emission Scanning electron microscopy (FESEM: Supra VP35 Carl Zeiss, Germany) and Stereo Zoom optical microscopy (Leica M 205A). The compressive strength of scaffolds was tested with an INSTRON tensile testing machine (model 3365, Instron Corp., UK) using a cross-head speed of 1mm/min with a maximum load of 30N load cell. Simple displacement technique was used to calculate the porosity and apparent density. A scaffold of weighing 'W' was immersed in a graded cylinder containing (V1) volume of water until no air bubble emerged from the scaffold. The total volume of the water and scaffold was then recorded as V2. Thus, the skeleton of the scaffold is (V2 - V1). On removing scaffold, the residual volume measured as V3. The apparent density of the scaffold ( $\rho$ ), was evaluated using,

$$\rho = \frac{W}{V_2 - V_3} \quad (2)$$

The porosity of the open pores in the scaffold ( $\epsilon$ ), was evaluated using,

$$\epsilon = \frac{V_1 - V_3}{V_2 - V_3} \quad (3)$$

Assessment of bioactivity was carried out by the standard in vitro procedure using analytical reagent-grade chemicals NaCl,  $\text{NaHCO}_3$ , KCl,  $\text{K}_2\text{HPO}_4 \cdot 3\text{H}_2\text{O}$ ,  $\text{MgCl}_2 \cdot 6\text{H}_2\text{O}$ ,  $\text{CaCl}_2$ , Tris-buffer,  $[\text{CH}_2(\text{OH})_3\text{CNH}_2]$ , and 1M HCl with ions concentrations. Samples were immersed in a cellular SBF at concentration of 0.01 g/ml in a clean glass beaker rinsed with HCl and deionized water. The bottles were placed inside a thermostated incubator at a temperature of 34°C while maintaining pH at 7.4. Throughout the period of immersion, the SBF solutions were not refreshed. The Schema of work of the fabricated scaffolds is shown in figure 1.

## 3. Results and discussion

The Optical zoom image of fabricated HA scaffold are shown in figure 1. XRD results of mono crystalline HA powder (figure 2) showed the hexagonal phase with  $p6/m$  symmetry as confirmed by a well-defined sharp  $d_{211}$  reflection peak at 31.74 [16]. The other prominent  $d_{300}$ ,  $d_{112}$ ,  $d_{002}$ ,  $d_{210}$ ,  $d_{202}$ ,  $d_{210}$  peaks corresponding to  $2\theta$  occurs at 32.89, 32.18, 25.86, 28.9, 34, 28.9 according to JCPDS Card no. 09-0432 confirms the pure HA phase. Thus, the hydro thermally synthesized HAP powder was highly stoichiometric and pure in HA phase. Exploiting scherer equation the crystallite size of the powder was found to be 43.9 nm and the percentage of crystallinity was found to be 1.39. The XRD pattern of scaffolds prepared by sponge technique using gum tragacanth as a binding agent for various sintering temperatures (1000 °C, 1500 °C and 2000 °C) is

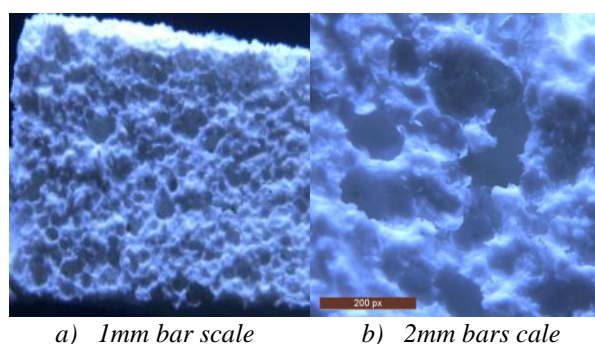


Fig. 1. Optical zoom image of fabricated HA scaffold

shown in fig.2. The stoichiometry of the synthesized HA powder used for the fabrication of scaffold plays a very important role in the phase purity of the sintered bodies. Ozekiet1 *al* [17] has emphasized the importance of the Ca/P ratio since any deviations from the stoichiometric value would have an unfavourable effect on the sintered properties of the hydroxyapatite body.

It can be observed that all the peak of the HA scaffold sintered at 1000 °C, 1500 °C and 2000 °C matches with the JCPDS Card no. 09-0432 for pure HA, throughout the sintering scheme employed. No decomposition products or other phases such as tricalcium phosphate(TCP), tetracalcium phosphate(TTCP) and calcium oxide(CaO) was not detected. For stoichiometric apatite powder C.-J. Liao *et.al* investigated the changes in XRD patterns of HA powder heated from 1000°C to 1500 °C. He reported no significant difference in XRD patterns from 1000°C – 1350°C for stoichiometric HA. No variation in XRD pattern of the scaffolds sintered at 1200 °C was observed, except for increase in the intensities of the diffraction peaks. Also, no additional peaks either due to gum, sponge or secondary phases was observed in XRD pattern. The intensities of the sintered scaffold improved with increase in sintering temperature. However, for non – stoichiometric hydroxyapatite, HAP starts to decompose by partial loss of OH- groups to form oxyhydroxyapatite (OHA) at nearly 800 °C [20].

The FTIR spectra of the HA scaffold fabricated using gaur gum as a binding agent, sintered at different temperatures is shown in figure 3a & 3b. In the FTIR spectra, the bands at 3570 and 630  $\text{cm}^{-1}$  are due to the contributions from hydroxyl stretching bands and bending bands of HA, respectively. The existence of the bending mode of absorbed water was not seen at elevated temperatures, hence no absorption bands were found in the range 3600 to 3300 $\text{cm}^{-1}$  for scaffolds sintered between 1100°C to 1200°C. The dehydroxylation is indicated by relative decrease in intensities of the OH vibration bands at 3700  $\text{cm}^{-1}$  and liberation/bending band at 630  $\text{cm}^{-1}$  as the sintering temperature increased from 1100°C to 1200°C. The bands at 1093 and 1041  $\text{cm}^{-1}$  were assigned to the components of the triply degenerate  $\nu_3$  antisymmetric P-O stretching mode, and the  $\nu_1$  P-O symmetric stretching mode was detected at 962  $\text{cm}^{-1}$ . Thus, the  $\nu_3$  and  $\nu_1$  antisymmetric and symmetric stretching modes decreased as the temperature was increased to 1200 °C. At 1200°C, the bands corresponding to OH groups were still present, but for temperatures above 1200°C (i.e 1250°C), figure (3b) the bands corresponding to OH groups were still present and the phosphate peak at 1093 and 1041 $\text{cm}^{-1}$  became broadened indicating the partial phase transformation to TTP and  $\beta$ -TCP during sintering [20].

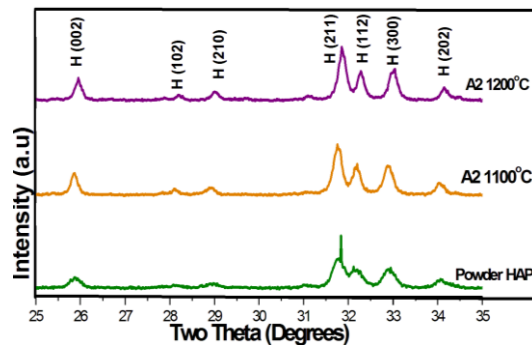


Fig 2. XRD pattern of pure HA powder and HA scaffold sintered at 1100 and 1200 °C

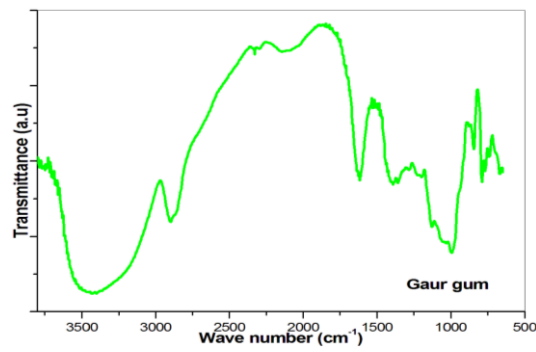


Fig 3a. FTIR spectra of the pure gaur gum

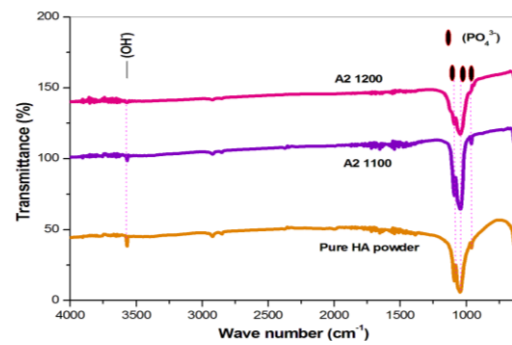


Fig 3b. FTIR spectra of the pure HA powder and HA scaffold A2 1100 and A2 1200

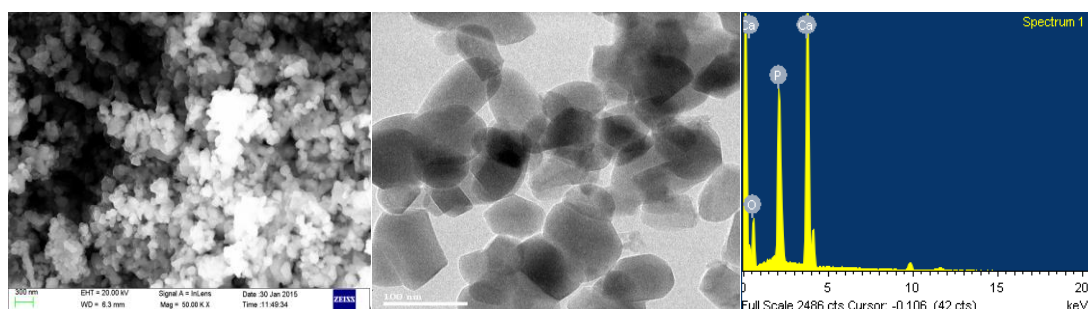


Fig 4. FESEM, HRTEM and EDAX spectrum of HA powder

The observations from TEM fig. 4 shows the Hydroxyapatite powders exploited to produce the macro porous scaffolds processed an elongated cylindrical shape with the crystallite size of 40 nm. The EDAX spectrum of HAP powder peeps the presence of the material constitution. The ratio of Calcium and Phosphate were found to be 1.68, very close to that of stoichiometric ratio of that of natural apatite (Fig. 4). The Stereo zoom microscope image (fig 1) and the FESEM images of the porous scaffold obtained using gaur gum as a binder, sintered at 1100°C, is shown in figure 6. The macro pores are open and interconnected with a diameter ranging from 500µm to 1000µm. Few studies have demonstrated an increase in osteogenesis with macro pore greater than 300 µm [23].

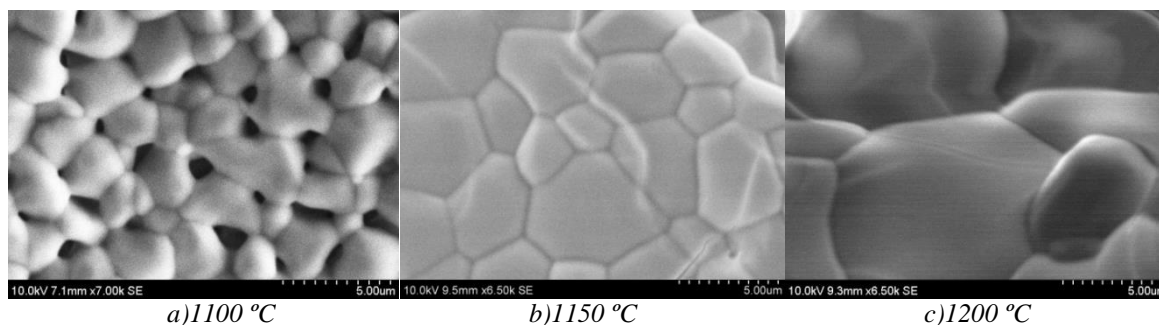


Fig 5. FESEM of HA scaffold sintered at a) 1100 °C; b) 1150 °C; c) 1200 °C

The samples labelled A2 1100 under FESEM showed highly interconnected micro pores of ~ 0.4 µm to 2 µm at 5 µm magnification as shown in figure 7, with 82.95 % porosity 0.82 g/cm<sup>3</sup> apparent density. The maximum yield strength for this sample was 0.35 MPa.

Table 1. Porosity, apparent density and maximum compression yield strength for HA scaffold samples

Concentration / Sintering Temperature	Label	Porosity (%)	Apparent density (g/cm <sup>3</sup> )	Max. Compression Yield Strength (MPa)
10wt% / 1100	A1 1100	84.35	0.82	0.27
10wt% / 1150	A1 1150	61.75	1.72	0.3
10wt% / 1200	A1 1200	47.12	1.86	0.42
15wt% / 1100	A2 1100	84.35	0.75	0.35
15wt% / 1150	A2 1150	64.25	1.83	1.1
15wt% / 1200	A2 1200	42.75	2.17	2.62

When the sintering temperature was raised to from 1100 °C to 1200 °C the pore strut walls got densified and noticeable decrease in pore size was experienced. The scaffolds fabricated using 10 wt% and 15 wt% gaur gum bonded scaffold labelled A1 and A2, when executed for compressive mechanical testing, using universal tensile testing machine are shown in table 1. For A2 samples the grain showed an increase from 1-2 µm to 10 – 12 µm with increase in sintering temperature and the maximum yield strength increased from 0.35 – 2.62 MPa. By Archimedes immersion technique, the measured porosity decreased from and 84.35% to 42.75 % and the apparent density increased from 0.82 to 4.75 g/cm<sup>3</sup> for A2 samples (Table 1).

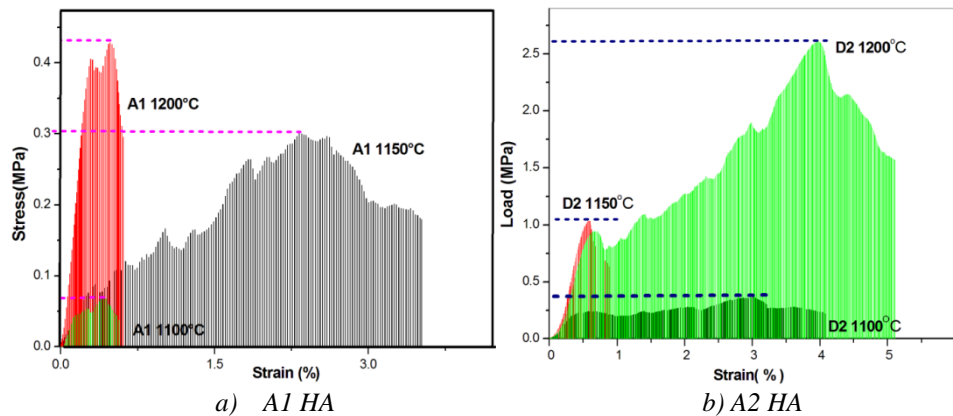


Fig 6. Stress - strain curve for a) A1 and b) A2 HA scaffold sintered at various temperatures

A typical stress - strain curve of the porous samples A1 and A2 sintered at 1100°C, and 1150°C and 1200°C are presented in Figure 6a,b for 10 wt% as well as 15 wt% binder concentration of gaur gum. The scaffolds were highly porous and the framework of the strut walls were broken even for smaller stress under compression. As the viscosity of the slurry was responsible for creating void spaces in the scaffold. Henceforth, in areas where HA slurry had not penetrated, the sintered samples had cavities due to complication aroused in impregnating the sponges with the slurry [24]. As the load increased, the force on framework exceeded the yield strength of the material resulting in a catastrophic failure as in brittle ceramic sample [25].

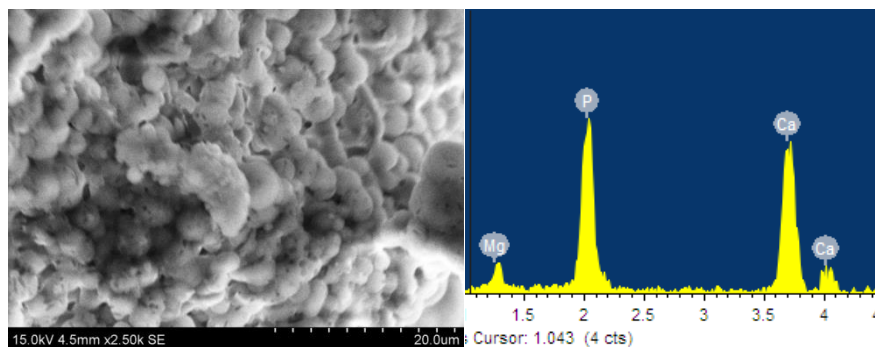


Fig. 7. SEM Image and EDAX spectrum of SBF

The sample A2 1100 following immersion for 7 days in SBF, apatite had almost completely colonized the surface of the scaffold (Fig 7). Traces of magnesium are found from EDAX after immersion for 7 days in SBF. The scaffold density is usually proportional to the maximum yield strength [15]. The compression yield strength of spongy bone is in the range of 0.2–4MPa, when the relative density is  $\sim 1.33\text{g/cm}^3$ . Interestingly our result was within this range and hence, can be constructively used in purpose to renovate of trabecular bone, in addition to seeding of cells in bone tissue engineering.

The size of the scaffold's grain increases by rising the sintering temperature. Consequently, the porosity decreased due to densification of the scaffold, intensifying the yield strength [1]. Hence, the scaffolds sintering temperature had a control on porosity as well as load bearing strength. The sample A1 corresponding to 5 wt% binder addition has the highest porosity of 84.35% synonymic to least compression strength of 0.32 MPa. Whereas, the samples A2 sintered at 1200°C has a higher load bearing capacity of 2.63 MPa compatible with 42.75 % porosity. Furthermore, in addition to the binder concentration the apparent density also has an impact on regulating the load bearing capacity of the material. The mechanical properties are firmly altered by apparent density [25]. In trabecular bone, the apparent density ranges from

0.14g/cm<sup>3</sup> to 1.10g/cm<sup>3</sup> [27]. The higher the apparent density elevated was its compression strength. Better susceptible scaffold with enhanced yield strength can be achieved by adding bioactive glass onto the initial ceramic slurry [27]. As a result, additives like SiC and SiO<sub>2</sub> powders were mixed in the optimized stable slurry to improve the material mechanical strength which can be as high as 16 MPa [29, 30]. The drawbacks of the polymer replication technique include weaker pore struts. Elements such as bio glasses or polymers help to improve pore strut thicknesses which enable to withstand higher compression stress [29 - 31]. It is found that mechanical properties varied with binder's concentration. The reduced hardness of gum tragacanth below 10 wt% created least load bearing ability, which can be accounted due to higher porosity. Moreover, the very lower load bearing ability may also be due to the presence larger porosity and lowered apparent density. Equilibrium between the porosity and density for a scaffold must be well-established for the precise objective; higher mechanical strength associates to higher density, while a high porosity do influence a surrounding favourable for living organism.

#### 4. Conclusions

In this study, porous scaffolds were processed using gaur gum, a natural gum used in food industry, in medicine, in pharmaceutical and also in adhesives. Polymeric sponge template method was furnished to assemble hydroxyapatite powder as porous scaffolds. The impact of gaur gum concentration on the preparation of scaffold proved to be successful. The scaffolds prepared with 15wt% gum concentrations at sintering temperature 1200°C proved that pure hydroxyapatite phase scaffolds with a maximum compressive yield strength of 2.62 MPa.

Density and porosity has a direct influence on the mechanical properties of HA scaffolds, which in turn depends on sintering temperature [30]. A further increase in temperature resulted in decomposition of Hydroxyapatite phase. Thus, Hydroxyapatite close to natural stoichiometric appetite is required to produce well-defined porous scaffolds with highly interconnected macro pores, suitable for bone implants, appropriate sintering encourages a better firing shrinkage of porous ceramics, which helps in deciding the mechanical properties of the scaffold.

#### Acknowledgement

This work was supported by DST – FIST under project number (SR-FIST-PSI-193-2014) Department of Physics, Sathyabama Institute of Science and Technology for providing the FT-IR and TGA facilities in characterizing the samples.

#### References

- [1] J.R. Woodard, A.J. Hilldore, S.K. Lan, C.J. Park, A.W. Morgan, J.A. Eurell, et al., *Biomaterials* **28**, 45 (2007).
- [2] S.K. Nandi, S. Roy, P. Mukherjee, *Indian J Med Res* **132**, 15 (2010).
- [3] Kensuke Kuroda and Masazumi Okido, *Hydroxyapatite Coating of Titanium Implants Using Hydroprocessing and Evaluation of Their Osteoconductivity*, *Bioinorganic Chemistry and Applications*, (2012), pp. 01.
- [4] S.Sai Nievethitha, N.Subhadrappa, Wei-Bor Tsai, N.Srinivasan, A.Moorthi, *International Journal of Biological Macromolecules* **98**, 67 (2017).
- [5] H. Maachoua, K.E. Balb, Y. Balb, A. Chagnesd, G. Coted, D. Alliouchea, *Trends Biomater. Artif. Organs*, **22**(1), 16(2008).
- [6] Yang Lei and Ning Xio Shan, *Trans. Nonferrous Met. Soc. China*, **15**(2), 257 (2005).
- [7] Mehdi Kazemzadeh Narnbat, Fariba Orang, Mehran Solati Hashtjin, *Iranian Biomedical Journal* **10**(4), 215 (2006).
- [8] Feng Wang, Enyan Guo, Enmin Song, Ping Zhao, Jinhua Liu, *Advances in Bioscience and Biotechnology* **1**, 185 (2010).

- [9] Md. JakirHossana, M. A Gafurb, M. R Kadirb, Mohammad MainulKarima, International Journal of Engineering & Technology **14**(1) 24 (2015).
- [10] J. Anita Lett, M. Sundareswari, K. Ravichandran, Materials Today: Proceedings **3**,1672 (2016).
- [11] J. Anita Lett, M. Sundareswari, K.Ravichandran, The role of cellulose in the formulation of macro and meso porous biocompatible Hydroxyapatite scaffolds, Mechanics, Materials Science & Engineering, April 2017 – ISSN 2412-5954
- [12] G. Daculsi, Biomaterials **19** (1998), pp. 1473—1478
- [13] Sunil Goswami, Dr. SonaliNaik, Journal of Scientific and Innovative Research **3**(1), 112 (2014).
- [14] Francesca Gervaso, Francesca Scalera, SanoshKunjalu Padmanabhan, High-Performance Hydroxyapatite Scaffolds for Bone Tissue Engineering Applications, Int. J. Appl. Ceram. Technol., (2011), pp. 1.
- [15] K.P. Sanosh, Min-Cheol Chu, A. Balakrishnan, Yong-Jin Lee, T.N. Kim, Current Applied Physics **9**, 1459 (2009).
- [16] Ozeki, Y. Fukui, H. Aoki, Applied Surface Science **253**, 5040(2007).
- [17] Chun-Jen-Liao, Feng-Huei Lin, Ko-Shao Chen, Jui-Sheng Sun, Biomaterials **20**, 1807 (1999).
- [18] Tan Chou Yong, Ramesh Singh, Sopyan, Teng Wan Dun, Sintering Behavior Of Hydroxyapatite Ceramics Prepared By Different Routes, The Am. Ceramics. Soc., Inc., 2009, pp. 127-138
- [19] Chandrasekhar Kothakali, M. Wei, A. Vasiliev a, M.T. Shaw, Acta Materialia **52**, 5655 (2004).
- [20] G. Muralithran, S. Ramesh, Ceramics International **26**,221 (2000).
- [21] Enobong R. Essien, LuqmanA. Adams, J. Chin. Chem. Soc. **63**, 001 (2016).
- [22] Y Kuboki; Q Jin; H Takita, The Journal of Bone and Joint Surgery. American **83**(1), 105 (2001).
- [23] C, Zhang Jun-yan, FU Yi-ming, ZENG Xiao-ming, Trans. Nonferrous Met. SOC. China, **16**, 453 (2006).
- [24] L. Montanaro, Y. Jorand, G. Fantozzi, A. Negro, Ceramic, J. Eur. Ceram. Soc. **18**, 1339 (1998).
- [25] L.A.Evans, D.J. Macey, J. Webb, Acanthopleurahirtosa, CalcifTissue Int. **51**, 78 (1992).
- [26] M. Kamitakahara, C. Ohtsuki, Y. Kozaka, S. Ogata, M. Tanihara, T. Miyazaki, Journal of the Ceramic Society of Japan **114**(1), **82**(2006).
- [27] N Monmaturapoj, C Yatongchai, Bull. Mater. Sci., December **34**(7)1733 (2011).
- [28] Hao-Yang Mi, Xin Jing, Max R. Salick, J Mater Sci **49**, 2324 (2014).
- [29] Xiao Huang and Xigeng Miao, Journal of Biomaterials Applications **21**(4), 351 (2007).
- [30] V.Karageorgiou, D.Kaplan, Biomaterials **26**(27), 5474 (2005).